PHYSICAL REVIEW A VOLUME 2, NUMBER 6 DECEMBER 1970

Transport Functions and Light Scattering in Simple Dense Fluids

Jean Pierre Boon* and Philippe Deguent
Faculté des Sciences, Université Libre de Bruxelles, Brussels, Belgium

(Received 1 May 1970)

The general expression for the transport coefficients at finite frequency is given by the spectral function of the autocorrelation of the flux corresponding to the transport phenomenon considered. Because the explicit analytical solution of such a correlation function involves the whole many-body problem for strongly coupled systems, appeal must be made to a model in order to derive the explicit frequency dependence of the transport functions. In the first part of this paper, we calculate these functions analytically [i.e., the diffusion $D(\omega)$, the viscosities $\eta_S(\omega)$ and $\eta_B(\omega)$, and the thermal conductivity $\kappa(\omega)$] from the generalized Berne-Boon-Rice model. The frequency dependence of these transport functions becomes significant at high frequencies, i.e., when ω approaches $\omega_c \sim \tau_c^{-1}$, where τ_c is the collision time, and should be essentially responsible for the departure from classical hydrodynamics. This is shown in Sec. II of this paper, where we present a calculation of the spectral distribution of the light scattered from thermal fluctuations in simple fluids. When the transport functions are introduced in the hydrodynamic equations to replace the usual constant transport coefficients, the spectrum of the scattered light is modified significantly, to second order in Γk^2, where Γ is essentially a linear function of the transport functions. The second-order spectrum obtained here is in agreement with previous results, but it is shown that the main effect arises from the frequency dependence of the transport functions, which was ignored in previous work. These effects induce a small but significant negative dispersion in the first-sound velocity. This prediction is in qualitative agreement with the recent light scattering experiments by Fleury and Boon on liquid argon, which were initially interpreted as a possible experimental observation of the frequency dependence of the transport functions in simple liquids.

I. INTRODUCTION

It is presently quite well established, from recent molecular dynamics *experiments*[1] and from neutron scattering data,[2] that classical monatomic liquids, e.g., argon, exhibit a dispersion curve in (ω, k) space, somewhat similar in shape to the well-known ^{4}He dispersion curve. However, it appears to be a very difficult task to develop a rigorous theory yielding a complete analytical description of the structure factor $S(k, \omega)$ in the whole (ω, k) space. Recent theoretical developments have been attempted in this direction, but practical computation still requires the introduction of model calculations.[3] A recent analysis of the linearized hydrodynamic modes by Résibois[4] may appear as a very elegant and fruitful starting point for further studies in this domain.

The dispersion curve $\omega(k)$ presents an inflection point for a value of k of the order of $k_c \sim 10^8$ cm^{-1}; this inflection may serve to separate the (ω, k) space roughly into two regions[1]: a low-k–low-ω region, characteristic of the collective modes, the hydrodynamic domain, and a high-k-high-ω region, or kinetic region, also called by some authors the domain of *generalyzed hydrodynamics*. In the present work, we are essentially concerned with that region of the (ω, k) space which can be denoted as the *intermediate region*, i.e., where at least one of the two variables ω and k can no longer be considered as tending to zero. In other words, if the hydrodynamic region is defined by

$$\lim \omega = 0, \quad \lim k = 0 \ , \tag{1.1}$$

and the *generalyzed hydrodynamics* domain by

$$\omega/\omega_c \sim 1, \quad k/k_c \sim 1, \tag{1.2}$$

where ω_c is the characteristic frequency of the order of the reciprocal collision time and k_c^{-1} is the characteristic wavelength of the order of the intermolecular distance, then the *intermediate region* is the domain where ω/ω_c and k/k_c are finite but small quantities. In this intermediate range the classical hydrodynamic approach is still valid, in so far as one accounts for the existence of not strictly zero values of ω and k. It is then expected that some new effects will be observed as small, but significant, deviations from classical hydrodynamics.

The situation where ω is taken in the hydrodynamic limit, i.e., $\omega \to 0$, while k becomes slightly larger than zero, has been considered recently by Foch on the basis of the Burnett equations.[5] In the present work we investigate the case where $k \ll k_c$ and ω/ω_c is finite but small, which corresponds to the physical situation of a light scattering experiment performed on a monatomic liquid.[6] Indeed, Fleury and Boon have recently carried out Brillouin-Mandelstam scattering experiments on liquid argon (as well as on liquid neon)[7] where they detected thermal phonons in the frequency range $\omega \sim 10^{10}$–

10^{11} cps. Since the collision time for simple liquids is of the order of 10^{-12}–10^{-13} sec, we have the ratio $\omega/\omega_c \sim 10^{-2}$, while k/k_c is an order of magnitude smaller ($\sim 10^{-3}$) which, as will be seen below, can be considered as satisfying the hydrodynamic limit $k \to 0$.

The general form of the linear transport coefficients at zero frequency is given by[8]

$$\sigma_0 = C \int_0^\infty dt\, \psi(t) \quad , \tag{1.3}$$

where C is a thermodynamic constant depending on the transport phenomenon considered and $\psi(t)$ is the autocorrelation function of the flux associated to the transport property. Now, at finite frequency, σ becomes ω dependent and is given by the spectral function $\tilde{\psi}(\omega)$, i.e., the *transport function* reads[9]

$$\sigma(\omega) = C \int_0^\infty dt\, e^{-i\omega t} \psi(t) \quad . \tag{1.4}$$

The transport function consists of two parts: a real (dissipative) part whose first term is merely σ_0 and an imaginary part, which accounts for the nondissipative part of the transport phenomenon. The latter contribution will become significant when ω approaches ω_c. In Sec. II, we present the general form of the different transport functions, namely, diffusion $D(\omega)$, viscosity $\eta(\omega)$, and thermal conductivity $\kappa(\omega)$.

However, it is easily recognized that the compact form of Eq. (1.4) involves the solution of the full many-body problem for (in the present case) strongly coupled systems. Therefore, for practical computation we need to introduce a model. In Sec. III, the expressions for the different transport functions are explicitly derived from a generalization of the Berne-Boon-Rice (BBR) model.[10] The interest of this computation follows, in particular, from the fact that the frequency dependence of the transport coefficients should appear as essentially responsible for the departure from classical hydrodynamics in the intermediate hydrodynamic range defined above by $k \to 0$, $\omega/\omega_c \sim 10^{-2}$.

In Sec. IV, we solve the linearized hydrodynamic equations,[11] where the usual transport coefficients are no longer constants, but have become the corresponding transport functions defined above, leading to a new dispersion equation. In the limit $\lim_{\omega\to 0}\sigma(\omega) = \sigma_0$, one obtains the roots, i.e., the poles determining the spectrum of the scattered light,[12] as presented in earlier work,[13] leading to the well-known spectrum consisting of three Lorentzians (the central Rayleigh component and the Brillouin-Mandelstam doublet).[14] Now, in the present case involving the transport functions $\sigma(\omega)$, we find a modified spectrum (Sec. V) whose main feature consists in the second-order effect on the Brillouin shift; we predict a negative dispersion for the hypersound propagation velocity. The modifications on the linewidths are also analyzed in Sec. VI. Finally, we present the evaluations for liquid argon, and compare our numerical results with experimental data; there is qualitative agreement between theory and experiment, as the hypersound velocities[7] seem to be systematically lower than the low-frequency values.[15] However, the smallness of the effect precludes quantitative conclusions as well as analysis of the linewidths. These points should be reexamined in the near future, with greater experimental accuracy.

II. TRANSPORT FUNCTIONS

In this section, we briefly recall the general expression and some properties of the frequency-dependent linear transport coefficients.[9] For the sake of convenience, we define the transport function as the normalized transport coefficient at finite frequency[16]

$$\sigma_N(\omega) = \lim_{\epsilon\to 0} \tilde{\psi}_N(\epsilon + i\omega) \quad . \tag{2.1}$$

Here $\tilde{\psi}_N(\epsilon + i\omega)$ is the Laplace transform of the normalized autocorrelation function $\psi_N(t)$:

$$\psi_N(t) = \langle J(0)J(t)\rangle / \langle [J(0)]^2 \rangle \ , \tag{2.2}$$

where $J(t)$ is the flux corresponding to the transport property considered, and the brackets $\langle \cdots \rangle$ denote the ensemble average.

The normalization introduced here permits us to eliminate the constant C from the usual definition, Eq. (1.4). However, we shall mainly be concerned with the ratio

$$\sigma(\omega)/\sigma_0 = G(\omega) - iH(\omega) \quad , \tag{2.3}$$

where $G(\omega)$ is the normalized power spectrum

$$G(\omega) = \tilde{\psi}(0)^{-1} \int_0^\infty dt\, \psi(t) \cos(\omega t) \quad , \tag{2.4}$$

and $H(\omega)$ is the corresponding sine Fourier transform

$$H(\omega) = \tilde{\psi}(0)^{-1} \int_0^\infty dt\, \psi(t) \sin(\omega t) \quad . \tag{2.5}$$

Notice that the normalization procedure also leads to a consistent definition for the transport coefficients since they are now all expressed as reciprocal frequencies.

The detailed spectrum of the transport functions, Eq. (2.3), is not known explicitly, because this would require the knowledge of the exact analytical form of the autocorrelation function $\psi(t)$. However, some information can be obtained from the extreme ends of the spectrum.[9] For low frequencies ($\omega \ll \omega_c$), $\sigma_N(\omega)$ may be expanded in a power series in ω to yield

$$\sigma_N(\omega)\big|_{\omega\ll\omega_C} = \sigma_N(0) + \sum_{n=1}^{\infty} \frac{(-i\omega)^n}{n!} \tilde{\psi}_N^{(n)}(0) \ , \tag{2.6}$$

with

$$\tilde{\psi}_N^{(n)}(0)=\int_0^\infty dt\, t^n \psi_N(t) \quad , \qquad (2.7)$$

and where $\sigma_N(0)$ is the normalized transport coefficient at zero frequency, i.e., with Eq. (1.3),

$$\sigma_N(0)=C^{-1}\sigma_0/\langle [J(0)]^2\rangle \quad . \qquad (2.8)$$

The high-frequency behavior $(\omega \gg \omega_c)$ of $\sigma_N(\omega)$ is given by

$$\sigma_N(\omega)\big|_{\omega\gg\omega_c}=\sum_{n=0}^{\infty}(i)^{2n}(i\omega)^{-2n-1}\langle [J^{(n)}(0)]^2\rangle/\langle [J(0)]^2\rangle \quad , \qquad (2.9)$$

with the moments

$$J^{(n)}(0)=(i\mathcal{L})^n J(0) \quad , \qquad (2.10)$$

where $\mathcal{L}$ is the Liouville operator. One observes that $\sigma_N(\omega \gg \omega_c)$ becomes purely imaginary, characterizing in this way the nondissipatedness of the high-frequency transport process. Notice that Eq. (2.9) can be computed in practice, since all we need to evaluate is $\langle [\dot{J}(0)]^2\rangle$, $\langle [\ddot{J}(0)]^2\rangle$, ..., which quantities can be calculated without great difficulty.

TABLE I. Analytic expressions of the coefficients for the transport functions, Eqs. (2.3), (3.6), and (3.7).

	a^2	$\sigma_N(0)$
D	$\dfrac{\langle \nabla^2 V\rangle}{m}$	$\dfrac{mD^0}{k_B T}$
η_S	$\dfrac{\langle [\dot{J}^{xy}(0)]^2\rangle}{\langle [J^{xy}(0)]^2\rangle}$	$\dfrac{\Omega k_B T \eta_S^0}{\langle [J^{xy}(0)]^2\rangle}$
η'	$\dfrac{\langle \dot{J}^{xx}(0)\dot{J}^{yy}(0)\rangle}{\langle J^{xx}(0)J^{yy}(0)\rangle}$	$\dfrac{\Omega k_B T(\eta_B^0-\frac{2}{3}\eta_S^0)}{\langle J^{xx}(0)\, J^{yy}(0)\rangle}$
η	$\dfrac{\langle [\dot{J}^{xx}(0)]^2\rangle}{\langle [J^{xx}(0)]^2\rangle}$	$\dfrac{\Omega k_B T(\frac{4}{3}\eta_S^0+\eta_B^0)}{\langle [J^{xx}(0)]^2\rangle}$
κ	$\dfrac{\langle [\dot{J}^{E}(0)]^2\rangle}{\langle [J^{E}(0)]^2\rangle}$	$\dfrac{3\Omega k_B T^2 \kappa^0}{\langle [J^{E}(0)]^2\rangle}$

III. MODEL TRANSPORT FUNCTIONS

In the present work, we are interested in the intermediate region, as defined in Sec. I. Although the frequencies involved here are much higher than those encountered in the usual hydrodynamic region, the intermediate domain is nevertheless in the low-frequency range of the spectrum, where computation of the transport functions is a very hard task, which requires the solution of Eqs. (2.6) and (2.7). Since the exact analytical form of $\psi(t)$ is not known, we introduce a model which merely consists in a generalization of the model initially developed by BBR, for the velocity autocorrelation function.[10] Consider the master equation governing the evolution of the autocorrelation function $\psi_N(t)$

$$\dot{\psi}_N(t)=-\int_0^t d\tau\, K(\tau)\psi_N(t-\tau) \quad , \qquad (3.1)$$

where we introduce the following ansatz for the kernel $K(t)$:

$$K(t)=a^2 e^{-b|t|} , \qquad (3.2)$$

with

$$a^2=K(0)=\langle [\dot{J}(0)]^2\rangle/\langle [J(0)]^2\rangle \quad , \qquad (3.3)$$

$$b=a^2/\tilde{K}(0)=a^2\sigma_N(0)=C^{-1}\sigma_0\langle [\dot{J}(0)]^2\rangle(\langle [J(0)]^2\rangle)^{-2} \quad . \qquad (3.4)$$

The BBR exponential model has been shown[10] to provide quite good results for the evaluation of the velocity autocorrelation function; in particular, it leads to very satisfactory agreement between the theoretical and experimental power spectra of $\psi(t)$ [namely, in this case, the diffusion function $D(\omega)$], especially for not too high frequencies (e.g., $\omega/\omega_c \sim 10^{-2}$). As the BBR model presents the advantage of analytical simplicity, we have generalized the exponential model to describe the general transport functions. These are now calculated in a straightforward manner from the expressions given above. From Eqs. (2.1) and (3.1)

$$\sigma_N(\omega)=[i\omega+\tilde{K}(\omega)]^{-1} \quad ; \qquad (3.5)$$

using Eqs. (2.3)–(2.5) and (3.2)–(3.4), we obtain

$$G(\omega)=\{[1-(\omega/a)^2]^2+[\sigma_N(0)\omega]^2\}^{-1} \quad , \qquad (3.6)$$

$$H(\omega)=G(\omega)\{[\sigma_N(0)-1/a^2\sigma_N(0)]\omega+\omega^3/a^4\sigma_N(0)\} , \qquad (3.7)$$

where a^2 and $\sigma_N(0)$ are given by Eqs. (3.3) and (2.8), respectively. The specific expressions for a^2 and $\sigma_N(0)$ for the different transport properties are displayed in Table I. Here we have chosen to consider the first (or shear) viscosity η_S; the second (or dilatational) viscosity $\eta' \equiv \eta_B - \frac{2}{3}\eta_S$ (with η_B, the bulk viscosity); the total viscosity $\eta \equiv \frac{4}{3}\eta_S+\eta_B$; and the thermal conductivity κ, because these are the quantities which appear in the hydrodynamic equations of Sec. IV. For the sake of completeness, the expressions for the diffusion D are also given in Table I. The expressions for the generalized forces, $\dot{J}^{\mu\nu}(\mu,\nu=x,y)$ for the viscosities and $\dot{J}^E$ for the thermal conductivity, as well as the quantities $\langle J^{\mu\nu}(0)J^{\mu\nu}(0)\rangle$ and $\langle [J^E(0)]^2\rangle$ are given explicitely in the Appendix.[17] The other symbols used in Table I are Ω for the volume, m for the mass, T for the temperature, k_B for the Boltzmann constant, and V for the pair potential energy of the system. Furthermore, D^0, η_S^0, η_B^0, and κ^0 denote the usual transport coefficients at zero frequency. All these quantitites are known, i.e., they can be calculated or obtained from experimental data; therefore, the functions $G(\omega)$ and $H(\omega)$ [Eqs. (3.6) and (3.7)] can be evaluated explicitly for the different transport functions.

IV. HYDRODYNAMIC MODES

Consider the Laplace-Fourier transformed linearized hydrodynamic equations,[4,11,18]

$$s\tilde{\rho}_k(s)+i\vec{k}\cdot\tilde{\vec{j}}_k(s)=\rho_k(0) \quad , \tag{4.1}$$

$$[s+k^2\tilde{v}(s)]\tilde{\vec{j}}_k(s)+i\vec{k}(c_0^2/\gamma)\tilde{\rho}_k(s)+i\vec{k}(c_0^2/\gamma)\beta\tilde{g}_k(s)=\vec{j}_k^{(0)} \quad , \tag{4.2}$$

$$[s+q^2\tilde{v}'(s)]\tilde{\vec{j}}_q^{(1)}(s)=\vec{j}_q^{(1)}(0) \quad , \tag{4.3}$$

$$[s+q^2\tilde{v}'(s)]\tilde{\vec{j}}_q^{(2)}(s)=\vec{j}_q^{(2)}(0) \quad , \tag{4.4}$$

$$[s+k^2\tilde{\lambda}(s)]\tilde{g}_k(s)+i\vec{k}[(\gamma-1)/\beta]\cdot\tilde{\vec{j}}_k(s)=g_k(0) \quad . \tag{4.5}$$

Here the quantities $\tilde{x}_k(s)$ denote the Laplace-Fourier transforms of the fluctuations $\delta x(\vec{r},t)$, e.g.,

$$\tilde{\rho}_k(s)=\int_0^\infty dt\, e^{-st}\int d\vec{r}\, e^{i\vec{k}\cdot\vec{r}}\delta\rho(\vec{r},t) \quad , \tag{4.6}$$

with the complex Laplace variables $s=\epsilon+i\omega$; while $\vec{j}_k$, $\vec{j}_q^{(i)}(i=1,2)$, and g_k represent the longitudinal current, the transverse current, and the heat current, respectively:

$$\vec{j}_k(t)=\rho_0\int d\vec{r}\,\vec{v}(t)e^{i\vec{k}\cdot\vec{r}} \quad , \tag{4.7}$$

$$\vec{j}_q(t)=\rho_0\int d\vec{r}\,\vec{v}(t)e^{i\vec{q}\cdot\vec{r}} \quad , \tag{4.8}$$

with

$$\vec{k}\cdot\vec{j}_q=0 \quad \text{or} \quad \nabla\cdot\vec{j}_\perp=0 \quad , \tag{4.9}$$

$$\vec{q}\cdot\vec{j}_k=0 \quad \text{or} \quad \nabla\cdot\vec{j}_\parallel=0 \quad , \tag{4.10}$$

$$g(\vec{r},t)=\rho_0\delta T(\vec{r},t) \quad . \tag{4.11}$$

The other quantities appearing in the linearized hydrodynamic equations are the following: c_0, the low-frequency limit of the first sound velocity; $\gamma=c_p/c_v$, the ratio of the specific heats; and $\beta=-(\partial\rho/\partial T)_P/\rho_0$, the coefficient of thermal expansion. $\tilde{v}(s)$, $\tilde{v}'(s)$, and $\tilde{\lambda}(s)$ are the transport functions corresponding, respectively, to the kinematic viscosities $v=\eta/\rho_0$, $v'=\eta_S/\rho_0$, and to the thermometric conductivity $\lambda=\kappa/\rho_0c_v$.

From the set of Eqs. (4.1)–(4.5) it is straightforward to obtain the following dispersion equation:

$$\begin{pmatrix} s & i\vec{k} & 0 & 0 & 0 \\ i\vec{k}c_0^2/\gamma & s+k^2\tilde{v}(s) & i\vec{k}(c_0^2/\gamma)\beta & 0 & 0 \\ 0 & i\vec{k}(\gamma-1)/\beta & s+k^2\tilde{\lambda}(s) & 0 & 0 \\ 0 & 0 & 0 & s+q^2\tilde{v}'(s) & 0 \\ 0 & 0 & 0 & 0 & s+q^2\tilde{v}'(s) \end{pmatrix}=0 \tag{4.12}$$

The two shear modes

$$s_{i=1,2}=-q^2\tilde{v}'(s) \tag{4.13}$$

may be immediately separated off, and we shall not consider them in more detail subsequently, since such modes have not been observed in simple liquids to date. Thus, the dispersion equation which remains to be solved for the three other modes is

$$s^3+s^2[\tilde{v}(s)+\tilde{\lambda}(s)]k^2+[c_0^2k^2+\tilde{v}(s)\tilde{\lambda}(s)k^4]s$$
$$+(c_0^2/\gamma)\tilde{\lambda}(s)k^4=0 \quad , \tag{4,14}$$

where the transport functions reduce to

$$\sigma(\omega)=\lim_{\epsilon\to 0}\tilde{\sigma}(s) \tag{4.15}$$

according to Eq. (2.1). Now, from Eqs. (2.3), (3.6), and (3.7), it is easily seen that to the lowest order in ω, the transport functions are

$$v(\omega)=v_0(1-i\alpha_v\omega) \quad , \tag{4.16}$$

$$\lambda(\omega)=\lambda_0(1-i\alpha_\lambda\omega) \quad , \tag{4.17}$$

with

$$v_0=(\tfrac{4}{3}\eta_S^0+\eta_B^0)/\rho_0 \quad , \tag{4.18}$$

$$\lambda_0=\kappa_0/\rho_0c_v \quad , \tag{4.19}$$

$$\alpha_v=\frac{\Omega k_BTv_0\rho_0}{\langle[J^{xx}(0)]^2\rangle}-\frac{\{\langle[J^{xx}(0)]^2\rangle\}^2}{\Omega k_BTv_0\rho_0\langle[\dot{J}^{xx}(0)]^2\rangle} \quad , \tag{4.20}$$

$$\alpha_\lambda=\frac{3\Omega k_BT^2\kappa_0}{\langle[J^E(0)]^2\rangle}-\frac{\{\langle[J^E(0)]^2\rangle\}^2}{3\Omega k_BT^2\kappa_0\langle[\dot{J}^E(0)]^2\rangle} \quad . \tag{4.21}$$

Since the α's are of the order of ω_c^{-1}, the first-order approximation [Eqs. (4.16) and (4.17)] is certainly appropriate to describe the intermediate region considered here, where $\omega/\omega_c \sim 10^{-2}$. It is now a matter of simple but lengthy, algebra to solve the dispersion equation (4.14)[19]; we, therefore, merely quote the results

$$s=-\Gamma_p^0k^2(1-\delta_1) \quad , \tag{4.22}$$

$$s=\pm ic_0k(1-\delta_2)-\Gamma_s^0k^2(1-\delta_3) \quad , \tag{4.23}$$

with

$$\Gamma_p^0 = \lambda_0/\gamma \quad , \tag{4.24}$$

$$\Gamma_s^0 = \tfrac{1}{2}\{\nu_0 + [(\gamma-1)/\gamma]\lambda_0\} \quad , \tag{4.25}$$

$$\delta_1 = (\gamma-1)(\gamma\nu_0/\lambda_0 - 1)(\Gamma_p^0 k/c_0)^2 \quad , \tag{4.26}$$

$$\delta_2 = \alpha_s(\Gamma_s^0 k/c_0) + \tfrac{1}{2}(\Gamma_s^0 k/c_0)^2 - \tfrac{1}{2}\delta_1 \quad , \tag{4.27}$$

$$\delta_3 = \alpha_s(\Gamma_s^0 k/c_0) + (\alpha_s + \alpha_l)(\Gamma_p^0 k/c_0) - (\tfrac{1}{2}\gamma\nu_0/\Gamma_s^0 - 1)(\Gamma_p^0 k/c_0)^2 \quad , \tag{4.28}$$

$$\alpha_s = \frac{c_0 k}{2\Gamma_s^0}\left(\frac{(1-\gamma)}{\gamma}\alpha_\lambda\lambda_0 - \alpha_\nu\nu_0\right) \quad ; \quad \alpha_l = c_0 k \alpha_\lambda \, . \tag{4.29}$$

Equation (4.22) represents the diffusion mode, arising from density fluctuations at constant pressure, and Eq. (4.23) represents the two (shifted) propagation modes, corresponding to the density fluctuations at constant entropy. It is easily recognized that the "high"-frequency effects arising from the nondissipative part of the transport functions appear in those terms containing the factors α, while the other correction terms represent pure second-order effects. It should be noticed that the latter are the only corrections which affect the diffusion mode,[20] whereas the frequency, as well as the lifetime of the thermal phonons, is also modified by the frequency effects. This will be discussed in more detail in Secs. V and VI.

V. SPECTRAL DISTRIBUTION

The spectral distribution of the light scattered from thermal fluctuations in a simple fluid is essentially given by the Van Hove correlation function,[21,22] introduced in Sec. I,

$$S(k,\omega) = 2\,\mathrm{Re}\,[\lim_{\epsilon\to 0}\langle\rho_{-k}(0)\tilde{\rho}_k(s)\rangle] \quad , \tag{5.1}$$

where the symbols ρ are used here to denote the density fluctuations, according to the definition given in Eq. (4.6). Solving the set of Eqs. (4.1), (4.2), and (4.5) for $\tilde{\rho}_k(s)$ yields

$$\tilde{\rho}_k(s) = M^{-1}\rho_k(0)\{s^2 + s[\tilde{\nu}(s) + \tilde{\lambda}(s)]k^2 + \tilde{\nu}(s)\tilde{\lambda}(s)k^4 + c_0^2 k^2(1-\gamma^{-1})\} \quad , \tag{5.2}$$

where M is the left-hand side of the dispersion equation (4.14). In Eq. (5.2) we have omitted the terms involving $\vec{j}_k(0)$ and $g_k(0)$, because they are thermodynamically independent of $\rho_k(0)$ and will therefore vanish by constructing the correlation function $S(k,\omega)$, which is the next step to be performed to obtain the spectral distribution. From Eq. (5.1) with Eqs. (5.2) and (4.14), combined with the results of Sec. IV, one finds

$$\begin{aligned}\frac{S(k,\omega)}{S(k)} = {} & \left(1-\frac{1}{\gamma}\right)(1+\theta_1)\frac{2\Gamma_p^0 k^2(1-\delta_1)}{[\Gamma_p^0 k^2(1-\delta_1)]^2+\omega^2} + \frac{1}{\gamma}(1+\theta_2)\left(\frac{\Gamma_s^0 k^2(1-\delta_3)}{[\Gamma_s^0 k^2(1-\delta_3)]^2+[\omega+c_0k(1-\delta_2)]^2}\right. \\ & \left. + \frac{\Gamma_s^0 k^2(1-\delta_3)}{[\Gamma_s^0 k^2(1-\delta_3)]^2+[\omega-c_0k(1-\delta_2)]^2}\right) + \frac{1}{\gamma}\theta_3\left(\frac{\omega+c_0k(1-\delta_2)}{[\Gamma_s^0 k^2(1-\delta_3)]^2+[\omega+c_0k(1-\delta_2)]^2}\right. \\ & \left. - \frac{\omega-c_0k(1-\delta_2)}{[\Gamma_s^0 k^2(1-\delta_3)]^2+[\omega-c_0k(1-\delta_2)]^2}\right) \quad ,\end{aligned} \tag{5.3}$$

with $S(k)$, the static structure factor,

$$S(k) = \langle\rho_{-k}(0)\rho_k(0)\rangle \quad , \tag{5.4}$$

which is discussed in great detail in the literature.[2] In Eq. (5.3) we have

$$\theta_1 = 2\alpha_s(\Gamma_s^0 k/c_0) + (\gamma - 3 + 2\gamma\nu_0/\lambda_0)(\Gamma_p^0 k/c_0)^2 \quad , \tag{5.5}$$

$$\theta_2 = 2\alpha_s(\Gamma_s^0 k/c_0) + \gamma\alpha_l(\Gamma_p^0 k/c_0) - (\gamma-1)(\gamma - 3 + 2\gamma\nu_0/\lambda_0)(\Gamma_p^0 k/c_0)^2 \quad , \tag{5.6}$$

$$\theta_3 = (\Gamma_s^0 k/c_0) + (\gamma-1)(\Gamma_p^0 k/c_0) + O(\Gamma_i^0 k/c_0)^3 \, , \qquad i = s, p \; . \tag{5.7}$$

The calculation presented here is valid to the second order in $(\Gamma_i^0 k/c_0)$, and we may therefore ignore the last term in Eq. (5.7). It is easily recognized that neglecting all the correction terms in Eq. (5.3) – namely, putting $\delta_j = 0$, and $\theta_j = 0$, $j = 1, 2, 3$ – leads to the simple usual expression for the spectral distribution in the hydrodynamic limit.[12] Furthermore, if one simply ignores the frequency dependence of the transport functions, i.e., setting $\alpha_\nu = \alpha_\lambda = 0$, one retrieves the spectrum involving the second-order terms.[13] These different effects are illustrated in Fig. 1, where they are considerably amplified for practical purposes. In particular, we observe a slight departure from the Lorentzian shape of the Brillouin lines. This will be discussed in detail in Sec VI., where we also present numerical evaluations of these effects for liquid argon.

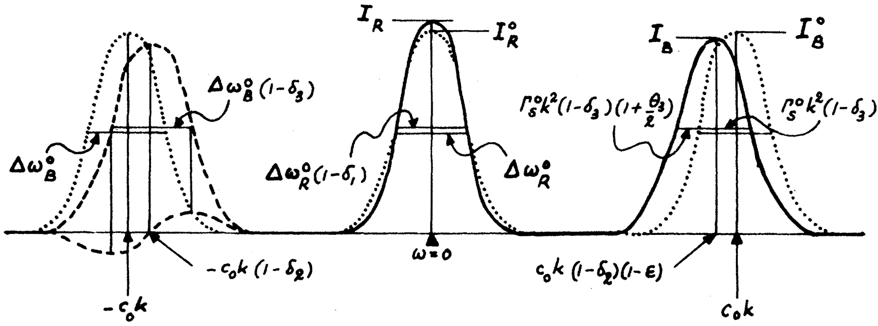

FIG. 1. Spectrum of the scattered light [full lines, Eq. (5.3)]. The dotted curves represent the "classical" spectrum (to the lowest order in k). The effects inducing changes in the Brillouin lines are decomposed and illustrated for the Stokes line by the dashed curves.

VI. DISCUSSION

In order to discuss the modifications introduced by frequency effects and second-order effects to the "classical" spectrum of the scattered light, as depicted in Fig. 1, we calculate the spectral characteristics: the frequency shift, the linewidths, and the intensities ratio. More precisely, we shall essentially be concerned with the relative changes introduced with respect to the first-order spectrum, whose characteristic quantities will be denoted by a superscript 0. We also present the numerical evaluations for argon in the normal liquid range, i.e., 85–100 °K, along the liquid-vapor equilibrium curve, which are the conditions under which the Fleury-Boon experiments have been performed.[1]

Let us first consider the central component. The Rayleigh line is a Lorentzian, centered around the incident frequency ω_0, i.e., around $\omega=\omega_s-\omega_0=0$ (with ω_s, the frequency of the scattered light) in Fig. 1, with a total linewidth

$$\Delta\omega_R=\Delta\omega_R^0(1-\delta_1) \quad , \tag{6.1}$$

where

$$\Delta\omega_R^0=4\Gamma_p^0 k^2 \quad . \tag{6.2}$$

In comparison with the classical result, one thus observes a slight narrowing, which is indebted to second-order effects [see Eq. (4.26)], and which is actually impossible to detect for liquid argon. Indeed, the evaluation of δ_1 yields

$$(\Delta\omega_R-\Delta\omega_R^0)/\Delta\omega_R^0\sim-10^{-5} \quad . \tag{6.3}$$

Consequently, there is also a slight increase of the peak intensity

$$I_R/I_R^0=(1+\theta_1)/(1-\delta_1) \quad , \tag{6.4}$$

with

$$I_R^0=2(1-\gamma^{-1})/(\Gamma_p^0 k^2) \quad , \tag{6.5}$$

which in the case of liquid argon gives

$$(I_R-I_R^0)/I_R^0\sim4\times10^{-6} \quad . \tag{6.6}$$

Since the Lorentzian is a normalized function, the integrated intensity is modified by θ_1 alone. One finds

$$\mathcal{I}_R=2(1-\gamma^{-1})(1+\theta_1)/\pi \quad . \tag{6.7}$$

Similarly for the Brillouin lines, since the second-order contributions – i.e., the two last terms in Eq. (5.3), represented in Fig. 1 for the Stokes line by the S-shaped dashed curve – vanish by integration, one obtains

$$2\mathcal{I}_B=2\gamma^{-1}(1+\theta_2)/\pi \quad . \tag{6.8}$$

Hence, from Eqs. (6.7) and (6.8), the Landau-Placzck ratio is

$$\mathcal{I}_R/2\,\mathcal{I}_B=(\gamma-1)(1+\theta_1)/(1+\theta_2) , \tag{6.9}$$

which is evaluated for liquid argon to yield

$$\mathcal{I}_R/2\,\mathcal{I}_B=(\gamma-1)(1+7\times10^{-5}) \quad . \tag{6.10}$$

All these corrections are, of course, negligible, since they cannot be detected experimentally. However, the situation is somewhat different for the frequency shift of the Brillouin lines, which can be measured with a much better experimental accuracy. The position of the Brillouin lines is displaced by the action of two factors whose effects add to each other to pull the Brillouin lines toward the central component. This situation is illustrated in Fig. 1 for the Stokes line. The dotted Lorentzian, representing the usual shape of this component, centered at $\omega=-c_0k$, is first displaced by an amount equal to $(1-\delta_2)$, as expressed by the third term in Eq. (5.3). Simultaneously, one observes a slight broadening by an amount equal to $(1-\delta_3)$, with $\delta_3<0$. This first change, as will be seen below from Eq. (4.26), is represented by the dashed Lorentzian centered around $\omega=-c_0k(1-\delta_2)$. In addition, the last term in Eq. (5.3), shown in Fig. 1 as the S-shaped dashed curve, introduces a slight departure from the Lorentzian shape and as a consequence of this asymmetry induces an additional pulling towards the central component. The over-all effect is shown for the anti-Stokes line in Fig. 1.

To evaluate the frequency shift, we perform a standard extremum calculation which yields the frequency of the thermal phonons to be detected. We obtain

$$\omega_B = \pm c_0 k(1-\delta_2)(1-\epsilon), \tag{6.11}$$

with

$$\epsilon = \frac{3\theta_2^2+\theta_3^2}{2\theta_3}\;\frac{1-\delta_3}{1-\delta_2}\;\frac{\Gamma_s^0 k}{c_0}\;. \tag{6.12}$$

Correspondingly, the peak intensity reads

$$I_B = I_B^0\,(1+\theta_2+\theta^2)/(1-\delta_3)\;, \tag{6.13}$$

with

$$I_B^0 = (\gamma\,\Gamma_s^0 k^2)^{-1}, \tag{6.14}$$

$$\theta^2 = (\theta_3^4 - 9\theta_2^4)/4\theta_3^2, \tag{6.15}$$

and the Brillouin linewidth is given by

$$\Delta\omega_B = \Delta\omega_B^0(1-\delta_3), \tag{6.16}$$

with

$$\Delta\omega_B^0 = 2\Gamma_s^0 k^2 . \tag{6.17}$$

Now, to compute the frequency shift we first notice that to a good approximation we have

$$\epsilon \cong (\tfrac{1}{2}\theta_3)\,(\Gamma_s^0 k/c_0) = \epsilon^{(2)}, \tag{6.18}$$

as a consequence of the expressions for θ_2 and θ_3 [Eqs. (5.6) and (5.7)] and δ_2 and δ_3 [Eqs. (4.27) and (4.28)]. It is also important to note that δ_2 can be written as the sum of two contributions:

$$\delta_2 = \delta_2^{(\omega)} + \delta_2^{(2)}, \tag{6.19}$$

where the superscript (ω) denotes the term containing high-frequency effects, i.e., the term involving α_s in Eq. (4.27), while $\delta_2^{(2)}$ represents the other terms, which are purely second-order terms. Since $\epsilon^{(2)}$ is also a second-order contribution, we may therefore rewrite ω_B, Eq. (6.11), by separating out the frequency effect

$$\omega_B \cong \pm c_0 k(1-\delta_2^{(\omega)} - \delta^{(2)}), \tag{6.20}$$

with

$$\delta^{(2)} = \delta_2^{(2)} + \epsilon^{(2)} . \tag{6.21}$$

Evaluating these different contributions for liquid argon yields

$$\delta_2^{(\omega)} \simeq -1.8\times10^{-5}\;, \tag{6.22}$$

$$\delta_2^{(2)} \simeq +2.4\times10^{-5}\;, \tag{6.23}$$

$$\epsilon^{(2)} \simeq +2.4\times10^{-5}\;, \tag{6.24}$$

from which one finds for the hypersonic velocity at $\omega\sim 3\times10^{10}$ cps

$$v_s \equiv (\omega_B/k) \cong c_0(1-3\times10^{-5})\;. \tag{6.25}$$

In other words, the theory predicts a slight negative dispersion. Now, from their experiments on liquid argon,[1] Fleury and Boon obtain

$$(v_s - c_0)/c_0 \cong -5\times10^{-3}, \tag{6.26}$$

[with c_0, the low-frequency velocity (at 1.2 MHz)[15]], which is about the order of magnitude of the experimental error. Despite the fact that this uncertainty precludes quantitative conclusions, their result seems to be qualitatively significant because they observe a systematicaly lower value for v_s as compared to c_0, which difference does not seem to be indebted to any kind of experimental error. In this sense, the theoretical prediction (6.25) would be in qualitative agreement with the observation (6.26); however, in order to ascertain the existence of a negative dispersion at frequencies $\omega/\omega_c\sim 10^{-2}$, greater experimental accuracy would be highly desirable. The same requirement holds for measuring modifications to the linewidth of the Brillouin lines. From Eq. (6.16), one predicts for liquid argon

$$(\Delta\omega_B - \Delta\omega_B^0)/\Delta\omega_B^0 \sim +3\times10^{-5}\;. \tag{6.27}$$

It is interesting to notice that, while the total linewidth is modified by δ_3 alone, the half-linewidth, because of the asymetry induced by the second-order terms, is affected by θ_3 also. One obtains to first order

$$\tfrac{1}{2}\Delta\omega_B = \Gamma_s^0 k^2(1-\delta_3)(1\pm\tfrac{1}{2}\theta_3), \tag{6.28}$$

where the plus (minus) sign corresponds to the inner (outer) half of the Brillouin line. Notice that $\frac{1}{2}\theta_3 = \epsilon^{(2)}$ also corresponds to the amount by which the Brillouin line is shifted because of the second-order effects. As far as relative changes are concerned with respect to the classical spectrum, this departure from the usual Lorentzian shape of the Brillouin lines should be the most important effect. Indeed, we have

$$\tfrac{1}{2}\Delta\omega_B \simeq \tfrac{1}{2}\Delta\omega_B^0(1-\delta_3\pm\tfrac{1}{2}\theta_3), \tag{6.29}$$

with, for liquid argon,

$$\delta_3 \simeq -3\times10^{-5}\;, \tag{6.30}$$

$$\theta_3 \simeq 8\times10^{-2}; \tag{6.31}$$

hence, one finds

$$(\tfrac{1}{2}\Delta\omega_B - \tfrac{1}{2}\Delta\omega_B^0)/\tfrac{1}{2}\Delta\omega_B^0 \sim \pm\tfrac{1}{2}\%. \tag{6.32}$$

However, this effect also appears to be the most difficult one to measure experimentally, because it requires the accurate determination of the position of the peak and high precision in the measurement of the total linewidth. Consequently, in so far as deviations from classical hydrodynamics in the intermediate region are concerned, it appears that the most important measurable effect (at least with the presently available experimental techniques) is the frequency shift, i.e., the dispersion for the first-sound velocity.

ACKNOWLEDGMENTS

We are grateful to Dr. P. A. Fleury and Dr. G. Nicolis for helpful discussions, and to Professor I. Prigogine for his constant interest during the course of this work, which was sponsored in part by the Instituts Internationaux de Physique et de Chimie, founded by E. Solvay. We are also indebted to Professor S. Yip and Professor M. Nelkin for valuable comments on the manuscript.

APPENDIX: GENERALIZED FORCES

The momentum flux is given by

$$J^{\mu\nu}=\sum_{i=1}^{N}\frac{1}{m}p_i^{\mu}p_i^{\nu}+\sum_{i<j}R_{ij}^{\mu}F_{\cdot j}^{\nu}-\delta_{\mu\nu}P\Omega$$

$$-\delta_{\mu\nu}(E-\langle E\rangle)\left(\frac{\partial P\Omega}{\partial E}\right)_{N,\Omega}\quad(\mu,\nu=x,y)\quad,\qquad\text{(A1)}$$

where p_i^{μ} denotes the μ component of the momentum of particle i, $\delta_{\mu\nu}$ is the Kronecker δ, P is the pressure, E is the internal energy, R_{ij} is the distance between particles i and j, F_{ij} is the force between them, and the bracket denotes the canonical ensemble average. The other symbols are defined in the main text (see Sec. III). For the shear viscosity, one has

$$\langle[J^{xy}(0)]^2\rangle=\Omega k_BT\left[\rho k_BT+\tfrac{2}{15}\pi\rho^2\int_0^{\infty}dR\,g^{(2)}(R)\,\frac{d}{dR}\left(R^4\,\frac{dV(R)}{dR}\right)\right]\quad,\qquad\text{(A2)}$$

with ρ the number density, and $g^{(2)}(R)$ the radial distribution function; and for the total viscosity we have

$$\langle[J^{xx}(0)]^2\rangle=2\rho\Omega(k_BT)^2+\langle[\sum_{i<j}R_{ij}^xF_{ij}^x]^2\rangle-[\langle\sum_{i<j}R_{ij}^xF_{ij}^x\rangle]^2-\left(\frac{\partial P\Omega}{\partial E}\right)_{N,\Omega}\{\rho\Omega(k_BT)^2+[\langle\sum_{i<j}R_{ij}^xF_{ij}^x\sum_{k<e}V_{ke}\rangle$$

$$-\langle\sum_{i<j}R_{ij}^xF_{ij}^x\rangle\langle\sum_{k<e}V_{ke}\rangle]\}\quad,\qquad\text{(A3)}$$

where

$$\left(\frac{\partial P\Omega}{\partial E}\right)_{N,\Omega}=\{\rho\,\Omega(k_BT)^2+\langle\sum_{i<j}R_{ij}^xF_{ij}^x\sum_{k<e}V_{ke}\rangle-\langle\sum_{i<j}R_{ij}^xF_{ij}^x\rangle\langle\sum_{k<e}V_{ke}\rangle\}\Big/\{\tfrac{3}{2}\rho\Omega(k_BT)^2+[\langle(\sum_{k<e}V_{ke})^2\rangle-(\langle\sum_{k<e}V_{ke}\rangle)^2]\}\;.\qquad\text{(A4)}$$

The generalized forces $\dot{J}^{xx}$ and $\dot{J}^{xy}$ are

$$\dot{J}^{xx}=-\frac{1}{m}\sum_{i<j}[3p_{ij}^xA_{ij}+p_{ij}^{\alpha}B_{ij}^{\alpha}]\quad,\qquad\text{(A5)}$$

$$\dot{J}^{xy}=-\frac{1}{m}\sum_{i<j}p_{ij}^{\alpha}C_{ij}^{\alpha}\;.\qquad\text{(A6)}$$

Here the superscript α is subject to the usual summation convention for repeated indices, and we have

$$\vec{p}_{ij}=\vec{p}_i-\vec{p}_j\quad,\qquad\text{(A7)}$$

$$A_{ij}=-F_{ij}^x\quad,\qquad\text{(A8)}$$

$$B_{ij}^{\alpha}=R_{ij}^x\,\frac{\partial^2V_{ij}}{\partial R_{ij}^x\,\partial R_{ij}^{\alpha}}\quad,\qquad\text{(A9)}$$

$$C_{ij}^x=\frac{\partial V_{ij}}{\partial R_{ij}^y}+R_{ij}^y\,\frac{\partial^2V_{ij}}{\partial(R_{ij}^x)^2}\quad,\qquad\text{(A10)}$$

$$C_{ij}^y=2\,\frac{\partial V_{ij}}{\partial R_{ij}^x}+R_{ij}^x\,\frac{\partial^2V_{ij}}{\partial R_{ij}^x\partial R_{ij}^y}\quad,\qquad\text{(A11)}$$

$$C_{ij}^z=R_{ij}^y\,\frac{\partial^2V_{ij}}{\partial R_{ij}^x\partial R_{ij}^z}\quad.\qquad\text{(A12)}$$

The energy current is given by

$$\vec{J}^E=\sum_{i=1}^{N}\left[\frac{1}{2m}\,\vec{p}_i^{\,2}+\tfrac{1}{2}\sum_{j\neq i}V_{ij}\right]\vec{p}_i/m$$

$$+\frac{1}{2m}\sum_{i\neq j}\sum p_i^{\alpha}F_{ij}^{\alpha}\vec{R}_{ij}-h\sum_{i=1}^{N}\vec{p}_i/m\quad,\qquad\text{(A13)}$$

where h is the equilibrium enthalpy per particle. From (A13) one has

$$\langle[J^E(0)]^2\rangle=(1/m)\rho\Omega k_BT[\tfrac{15}{2}(k_BT)^2+(\langle h^{\alpha\beta}h^{\alpha\beta}\rangle$$

$$-\langle h^{\alpha\beta}\rangle\langle h^{\alpha\beta}\rangle)]\quad,\qquad\text{(A14)}$$

where $h^{\alpha\beta}$ is the potential contribution to the microscopic enthalpy per particle

$$h^{\alpha\beta}=\tfrac{1}{2}\sum_{j\neq i}(V_{ij}\delta_{\alpha\beta}+F_{ij}^{\alpha}R_{ij}^{\beta})\quad.\qquad\text{(A15)}$$

The corresponding generalized force reads

$$\dot{\vec{J}}^E=\vec{L}+\vec{M}+\vec{N}\quad,\qquad\text{(A16)}$$

$$\vec{L}=\sum_{i\neq j}\sum\left\{\vec{p}_i\left(\vec{p}_{ij}\cdot\frac{\partial V_{ij}}{\partial\vec{R}_{ij}}\right)-\vec{p}_{ij}\left(\vec{p}_{ij}\cdot\frac{\partial V_{ij}}{\partial\vec{R}_{ij}}\right)\right.$$

$$\left.-\vec{R}_{ij}\left[\vec{p}_{ij}\cdot\left(\vec{p}_i\,\frac{\partial^2V_{ij}}{\partial\vec{R}_{ij}\partial\vec{R}_{ij}}\right)\right]\right\}\quad,\qquad\text{(A17)}$$

$$\vec{\mathrm{M}}=\sum_{i\neq j}\sum\left((p_i^2\overleftrightarrow{\mathrm{I}}+2\vec{\mathrm{p}}_i\vec{\mathrm{p}}_i)\cdot\frac{\partial V_{ij}}{\partial\vec{\mathrm{R}}_{ij}}\right), \tag{A18}$$

$$\vec{\mathrm{N}}=\sum_{i=1}^{N}\sum_{j\neq i}\sum_{k\neq i}\left[m\vec{\mathrm{R}}_{ij}\left(\frac{\partial V_{ij}}{\partial\vec{\mathrm{R}}_{ij}}\cdot\frac{\partial V_{ik}}{\partial\vec{\mathrm{R}}_{ik}}\right)-mV_{ij}\frac{\partial V_{ik}}{\partial\vec{\mathrm{R}}_{ik}}\right]. \tag{A19}$$

---

[*] Chargé de Recherches au Fonds National de la Recherche Scientifique (F.N.R.S.) Belgium.

[1] A. Rahman, in *Neutron Inelastic Scattering* (IAEA, Vienna, 1968), Vol. 1, p. 561.

[2] For a general account, see, e.g., P. A. Egelstaff, *An Introduction to the Liquid State* (Academic, London, 1967); K. Sköld, in *Simple Dense Fluids*, edited by H. L. Frisch and Z. Salsburg (Academic, New York, 1968), pp. 119–182, and references therein. See also S. H. Chen, O. J. Eder, P. A. Egelstaff, B. C. G. Haywood, and F. J. Webb, Phys. Letters 19, 269 (1965); K. Sköld and K. E. Larsson, Phys. Rev. 161, 102 (1967).

[3] See the review chapter by P. Schofield, in *Physics of Simple Liquids*, edited by H. N. V. Temperley, J. S. Rowlinson, and G. S. Rushbrooke (North-Holland, Amsterdam, 1968), Chap. 13. See also R. Nossal, Phys. Rev. 166, 81 (1968); C. H. Chung and S. Yip, *ibid.* 182, 323 (1969); J. Hubbard and J. L. Beeby, J. Phys. C. 2, 556 (1969); A. Z. Akcasu and E. Daniels (unpublished); B. L. Clarke and S. A. Rice, Phys. Fluids 13, 271 (1970).

[4] P. Résibois, Phys. Letters 30A, 465 (1969); J. Stat. Phys. 2, 21 (1970).

[5] J. Foch, Phys. Fluids 11, 2336 (1968).

[6] The interesting low-momentum–high-energy region, i.e., the generalized hydrodynamic domain for which $k\to 0$ and $\omega/\omega_c\sim 1$ has recently been investigated by J. P. McTague, P. A. Fleury, and D. B. Dupré, Phys. Rev. 188, 303 (1969).

[7] P. A. Fleury and J. P. Boon, Phys. Rev. 186, 244 (1969).

[8] See, e.g., the review article by R. Zwanzig, Ann. Rev. Phys. Chem. 16, 67 (1965), and the references therein.

[9] R. Zwanzig, J. Chem. Phys. 43, 714 (1965); H. L. Frisch, Physics 2, 209 (1966); B. J. Berne, J. P. Boon, and S. A. Rice, J. Chem. Phys. 47, 2283 (1967); 48, 2833 (1968); P. C. Martin and S. Yip, Phys. Rev. 170, 151 (1968).

[10] B. J. Berne, J. P. Boon, and S. A. Rice, J. Chem. Phys. 45, 1086 (1966); see also R. C. Desai and S. Yip, Phys. Rev. 166, 129 (1968); P. C. Martin and S. Yip, *ibid.* 170, 151 (1968).

[11] See, e.g., F. V. Hunt, in *AIP Handbook*, edited by D. E. Gray (McGraw-Hill, New York, 1957), Chap. 3c, pp. 3–33.

[12] R. D. Mountain, Rev. Mod. Phys. 38, 205 (1966).

[13] R. D. Mountain and T. A. Litovitz, J. Acoust. Soc. Am. 42, 516 (1967); W. H. Nichols and E. F. Carome, J. Chem. Phys. 49, 1000 (1968); A. B. Bhatia and E. Tong, Phys. Rev. 173, 231 (1968).

[14] Actually, the Brillouin-Mandelstam lines exhibit a slight departure from Lorentzian shape, because of the second-order terms. (See Ref. 13, and Sec. V of the present paper).

[15] W. Van Dael, A. Van Itterbeek, A. Cops, and J. Thoen, Physica 32, 611 (1966).

[16] Connection between the usual definition of $\sigma(\omega)$ and its normalized expression $\sigma_N(\omega($ is explicitly given below; see Eq.)(2.8) and Table I.

[17] We are indebted to M. H. Ernst for his collaboration on the calculation of the analytical expression for the generalized forces as presented in the Appendix. See also R. Zwanzig and R. D. Mountain, J. Chem. Phys. 43, 4464 (1965).

[18] L. P. Kadanoff and P. C. Martin, Ann. Phys. (N.Y.) 24, 419 (1963).

[19] Equation is solved to the second order in zk/c_0, ($z=v_0$, λ_0); indeed although these second-order terms are small, they are not negligible with respect to the $\alpha\omega$ terms, Eqs. (4.16), and (4.17), as will be seen for the case of liquid argon in Sec. VI.

[20] Notice, however, that the intensity of the central component in the spectral distribution is affected by frequency effects, as seen from Eq. (5.3).

[21] L. I. Komarov and I. Z. Fisher, Zh. Eksperim. i Teor. Fiz. 43, 1927 (1962). [Soviet Phys. JETP 16, 1358 (1963)].

[22] G. B. Benedek, in *Statistical Physics, Phase Transitions, and Superfluidity*, edited by M. Chretien, S. Deser, and E. P. Gross (Gordon and Breach, New York, 1968), Vol. 2.